Transactions on Modelling and Simulation vol 11, © 1995 WIT Press, www.witpress.com, ISSN 1743-355X

Solution of one-phase solid-liquid phase change enthalpy equation by the dual reciprocity boundary element method

B. Šarler, A. Košir

Laboratory for Fluid Dynamics and Thermodynamics, Faculty of Mechanical Engineering, University of Ljubljana, Ljubljana, Slovenia

Abstract

This paper presents a solution to the entalpy equation corresponding to solid-liquid phase change systems by the dual reciprocity boundary element method. The physical model is based on the one-phase averaged formulation of incompressible distinct or continuous phase-change materials with temperature-dependent thermal conductivities and specific heats of the solid and liquid phases. The boundary-domain integral equation is structured by Green's function of the Laplace equation and by the dual reciprocity boundary representation of the domain integrals. Discretization in a two-dimensional cartesian frame is based on straight line boundary elements with constant space and linear time shape functions, and on global so-called first order radial interpolation functions. The convergence of the method with respect to discretization, Peclet and Stefan number is investigated by comparing the quasi-one-dimensional numerical solution with the one-dimensional exact solution.

Introduction

Various aspects of modern technology are related to the prediction of solid-liquid phase change phenomena. The modelling of transport phenomena represents an important share of this activity. An overview of this discipline can be found in [1]. A data base of relevant references including a glossary of key words is provided in [2].

When treating transport phenomena through the physical concept of continuum mechanics, the coupled microscopic conservation equations for energy, entropy, momentum, moment of momentum, and species have to be solved in the solid and in the liquid phase connected with the microscopic interfacial balances.

Due to the presence of complex interfacial structures that characterize solid-liquid phase change in most cases, it is impossible to predict macroscopic system characteristics by solving the described set of equations on the microscopic scale. Averaging has to be applied to the microscopic equations in order to be able to describe global system behaviour. These equations are then solved for averaged macroscopic quantities. Such two-phase averaged formulation [3] for solid-liquid phase change systems could be much simplified by neglecting the dispersive and phase-interphase terms and by adding the averaged conservation equations of one phase to the corresponding ones of the other phase. A one-phase averaged formulation is thus obtained. Models based on this for-

mulation [4] are advantageous because there are only half as many equations to solve as in two-phase models. Their main disadvantage is the fact that some of the quantities have to be assumed instead of calculated. The first discrete approximative solving of transient temperature, velocity and concentration fields based on one-phase solid liquid phase-change model was begun in the second part of the eighties by using the established finite volume method.

Due to the substantial advances [5] made in using the boundary element method in solving nonlinear transport phenomena models, great interest exists in using this method for coping with solid-liquid phase changes as well. A comprehensive survey of the related BEM efforts is published in [6].

The primary step towards solving one-phase solid liquid phase-change equations by the BEM has been achieved by rewriting them [7] into boundary-domain integral shape using structuring with the fundamental solution of the Fourier equation. This allows the solving of the derived boundary-domain integral equations by including the dual reciprocity conversion [8] of the domain integrals to boundary integrals. The calculations in the problem subsequently reduce to the integrations on the geometrical boundary of the considered system exclusively. This strategy was first applied for solving the conduction-governed Stefan problem [9] followed by a comparison with the results obtained by several finite element methods [10] for Rathjen and Jiji's rectangular corner freezing benchmark [11] and standards set in [12]. The comparison favoured BEM with respect to accuracy.

The two advantages, the boundary only character of the calculations and accuracy, have led the present authors to upgrade their previous research by considering both convective and conductive terms in the solid-liquid phase change averaged enthalpy conservation equation. The previous effort in applying the dual reciprocity boundary element method to convective-diffusive problems [13] provides useful support in achieving this goal.

Governing Equation

Consider a connected fixed domain Ω with boundary Γ occupied by a phase change material with density ρ_0, temperature dependent specific heat $c_{\mathcal{P}}$ and thermal conductivity $k_{\mathcal{P}}$ of the solid $\mathcal{P} = \mathcal{S}$ and the liquid $\mathcal{P} = \mathcal{L}$ phase, and specific fusion enthalpy of the solid-liquid phase change $h_{\mathcal{M}}$. The volume-averaged one-phase continuum formulation for enthalpy conservation in the assumed system is

$$\frac{\partial}{\partial t}(f_{\mathcal{S}}\, \rho_0\, h_{\mathcal{S}} + f_{\mathcal{L}}\, \rho_0\, h_{\mathcal{L}}) + \nabla \cdot (f_{\mathcal{S}}\, \rho_0\, \mathbf{V}_{\mathcal{S}}\, h_{\mathcal{S}} + f_{\mathcal{L}}\, \rho_0\, \mathbf{V}_{\mathcal{L}}\, h_{\mathcal{L}})$$
$$= -\nabla \cdot (f_{\mathcal{S}}\, \mathbf{F}_{\mathcal{S}} + f_{\mathcal{L}}\, \mathbf{F}_{\mathcal{L}}) + f_{\mathcal{S}}\, q_{\mathcal{S}} + f_{\mathcal{L}}\, q_{\mathcal{L}}, \quad f_{\mathcal{S}} + f_{\mathcal{L}} = 1. \tag{1}$$

Function $f_{\mathcal{P}}$ presents the temperature dependent volume fraction, $h_{\mathcal{P}}$ the specific enthalpy, $\mathbf{V}_{\mathcal{P}}$ the known solenoidal velocity, $\mathbf{F}_{\mathcal{P}}$ the heat flux, and $q_{\mathcal{P}}$ the heat source of phase $\mathcal{P}$. Pressure effects and viscous dissipation have been ignored. Heat sources could depend arbitrarily on temperature and independent time and position variables. Due to the local thermal equilibrium between the phases, the phase temperatures $T_{\mathcal{S}}$ and $T_{\mathcal{L}}$ are equal and denoted by the common symbol T. Constitutive equations for the two heat fluxes are based on the Fourier relation

$$\mathbf{F}_{\mathcal{S}} = -\, k_{\mathcal{S}}\, \nabla T, \quad \mathbf{F}_{\mathcal{L}} = -\, k_{\mathcal{L}}\, \nabla T, \tag{2}$$

and the enthalpy-temperature relationship is defined as

$$h_{\mathcal{S}} = h_{0\mathcal{S}} + \int_{T_h}^{T} c_{\mathcal{S}}(\theta)\, d\theta, \quad h_{\mathcal{L}} = h_{0\mathcal{L}} + \int_{T_h}^{T} c_{\mathcal{L}}(\theta)\, d\theta + h_{\mathcal{M}}, \tag{3}$$

with $h_{0\mathcal{P}}$ representing the specific enthalpy reference of phase $\mathcal{P}$ and T_h representing the enthalpy reference temperature.

The specific type of the solid liquid phase-change process is incorporated into equation (1) by prescribing the appropriate dependence $f_{\mathcal{P}}(T)$ and by providing the velocity of the liquid phase through the one-phase momentum equation. The velocity of the solid phase has to be prescribed. The liquid fraction function for the pure substance is modelled by the Heaviside step function centred around melting temperature $T_{\mathcal{M}}$. The linear variation from 0 to 1 from the solidus temperature $T_{\mathcal{S}}$ to the liquidus temperature $T_{\mathcal{L}}$ or some other, more sophisticated relation, is used in the case of multicomponent systems. The equiaxed type of solidification is modelled by $\mathbf{V}_{\mathcal{S}} = \mathbf{V}_{\mathcal{L}}$ and the columnar one with $\mathbf{V}_{\mathcal{L}} = \mathbf{V}$, $\mathbf{V}_{\mathcal{S}} = \mathbf{V}_{\text{sys}}$, where $\mathbf{V}_{\text{sys}}$ denotes the system velocity. The complete range of possible specific one-phase models is elaborated in [4].

Equation (1) is rewritten into boundary-domain integral shape by introducing the Kirchhoff variable

$$\mathcal{T} = T_{\mathcal{T}} + \int_{T_{\mathcal{T}}}^{T} \frac{k(\theta)}{k_0}\, d\theta = T + \int_{T_{\mathcal{T}}}^{T} \frac{k_{\mathcal{T}}(\theta)}{k_0}\, d\theta, \tag{4}$$

with $T_{\mathcal{T}}$ denoting the Kirchhoff variable reference temperature, and by weighting it over space-time $[\Omega] \times [t_0, t_0 + \Delta t]$ with the fundamental solution of the Laplace equation $T^*(\mathbf{p};\mathbf{s})$. After a lengthy procedure, detailed in [14], the following boundary-domain integral expression is obtained

$$\begin{aligned}
&\int_{\Omega} \rho_0\, c_0\, \mathcal{T}(\mathbf{p}, t_0 + \Delta t)\, T^*(\mathbf{p};\mathbf{s})\, d\Omega - \int_{\Omega} \rho_0\, c_0\, \mathcal{T}(\mathbf{p}, t_0)\, T^*(\mathbf{p};\mathbf{s})\, d\Omega \\
&\qquad + \int_{t_0}^{t_0+\Delta t} \int_{\Omega} \mathbf{\Lambda} \cdot \nabla \mathcal{T}\, T^*\, d\Omega\, dt \\
&\quad = \int_{t_0}^{t_0+\Delta t} \int_{\Gamma} k_0\, T^*\, \frac{\partial \mathcal{T}}{\partial n_{\Gamma}}\, d\Gamma\, dt - \int_{t_0}^{t_0+\Delta t} \int_{\Gamma} k_0\, \mathcal{T}\, \frac{\partial T^*}{\partial n_{\Gamma}}\, d\Gamma\, dt \\
&- \int_{t_0}^{t_0+\Delta t} c^*(\Omega, \mathbf{s})\, k_0\, \mathcal{T}(\mathbf{s}, t)\, dt + \int_{t_0}^{t_0+\Delta t} \int_{\Omega} \left[q + \Upsilon\, \frac{\partial \mathcal{T}}{\partial t} \right] T^*\, d\Omega\, dt;
\end{aligned}$$

$$\mathbf{\Lambda} = \rho_0\, \frac{k_0}{k} \left(\left[(1 - f_{\mathcal{L}})\, c_{\mathcal{S}} - \frac{df_{\mathcal{L}}}{dT}\, h_{\mathcal{S}} \right] \mathbf{V}_{\mathcal{S}} + \left[f_{\mathcal{L}}\, c_{\mathcal{L}} + \frac{df_{\mathcal{L}}}{dT}\, h_{\mathcal{L}} \right] \mathbf{V}_{\mathcal{L}} \right),$$

$$\Upsilon = \rho_0 \left[c_0 - \frac{k_0}{k} \left(c + h_{\mathcal{LS}}\, \frac{df_{\mathcal{L}}}{dT}\, \frac{\partial \mathcal{T}}{\partial t} \right) \right],$$

$$c^*(\Omega, \mathbf{s}) = -\int_{\Omega} \nabla^2 T^*(\mathbf{p};\mathbf{s})\, d\Omega, \quad T_2^*(\mathbf{p};\mathbf{s}) = \frac{1}{2\pi}\, \log \frac{r_0}{|\mathbf{p} - \mathbf{s}|}. \tag{5}$$

Function T_2^* stands for the two-dimensional planar symmetry form of the fundamental solution T^*. Position vectors of the field and source point are denoted by $\mathbf{p}$ and $\mathbf{s}$ respectively, and the normal on Γ by $\mathbf{n}_{\Gamma}$. The volume-averaged thermal conductivity k and the specific heat c are defined as

$$k = k_0 + k_{\mathcal{T}} = f_{\mathcal{S}}\, k_{\mathcal{S}} + f_{\mathcal{L}}\, k_{\mathcal{L}}, \quad c = c_0 + c_{\mathcal{T}} = f_{\mathcal{S}}\, c_{\mathcal{S}} + f_{\mathcal{L}}\, c_{\mathcal{L}}. \tag{6}$$

Constants k_0, c_0 denote mean values, and functions $k_{\mathcal{T}}$, $c_{\mathcal{T}}$ the temperature behaviour of the respective quantities.

We seek the solution of the governing equation for volume-averaged temperature at final time $t = t_0 + \Delta t$, where t_0 denotes the initial time and Δt the positive time increment.

Equation (5) is solved by the related Kirchhoff transformed initial and boundary conditions

$$\mathcal{T}(\mathbf{p},t_0) = T_{\mathcal{T}} + \int_{T_{\mathcal{T}}}^{T_0} \frac{k}{k_0}\, d\theta;\ \mathbf{p} \in \Omega \oplus \Gamma, \tag{7}$$

$$\mathcal{T}(\mathbf{p},t) = T_{\mathcal{T}} + \int_{T_{\mathcal{T}}}^{T_\Gamma} \frac{k}{k_0}\, d\theta;\ \mathbf{p} \in \Gamma^D, \tag{8}$$

$$-k_0 \frac{\partial \mathcal{T}}{\partial n_\Gamma}(\mathbf{p},t) = F_\Gamma;\ \mathbf{p} \in \Gamma^N, \tag{9}$$

$$-k_0 \frac{\partial \mathcal{T}}{\partial n_\Gamma}(\mathbf{p},t) = h_\Gamma \left(\mathcal{T}(\mathbf{p},t) - T_\Gamma - \int_{T_{\mathcal{T}}}^{T(\mathcal{T}(\mathbf{p},t))} \frac{k_T}{k_0}\, d\theta \right);\ \mathbf{p} \in \Gamma^R. \tag{10}$$

The initial conditions are defined with the known function T_0 and the boundary conditions of the Dirichlet, Neumann and Robin type are determined through the known functions T_Γ, F_Γ and h_Γ defined at the not necessarily connected parts Γ^D, Γ^N and Γ^R of the boundary Γ.

Numerical Implementation

The transformation of the domain integrals in equation (5) into boundary integrals is based on the Dual Reciprocity Method (DRM). In this method an arbitrary scalar valued function $\mathcal{F}(\mathbf{p},t)$ is approximated over the domain Ω with $n = 1, 2, \ldots, N$ global space interpolation functions $\Psi_n^p(\mathbf{p})$ and time shape functions $\Psi_n^t(t)$

$$\mathcal{F}(\mathbf{p},t) \approx \Psi_n^p(\mathbf{p})\, \Psi_n^t(t). \tag{11}$$

The Einstein summation is used in this text wherever possible. By defining the matrix Ψ_{nm}^p and its inverse $\tilde{\Psi}_{nm}^p$ with the positions of $m = 1, 2, \ldots, N$ points $\mathbf{p}_m$ distributed in $\Omega \oplus \Gamma$

$$\mathcal{F}(\mathbf{p}_m,t) = \Psi_{nm}^p\, \Psi_n^t(t), \quad \tilde{\Psi}_{nm}^p\, \Psi_{nm}^p = 1, \tag{12}$$

the time shape function $\Psi_n^t(t)$ is expressed through

$$\Psi_n^t(t) = \tilde{\Psi}_{nm}^p \mathcal{F}(\mathbf{p}_m,t). \tag{13}$$

By defining the harmonic functions $\hat{\Psi}_n^p$

$$\nabla^2 \hat{\Psi}_n^p(\mathbf{p}) = \Psi_n^p(\mathbf{p}), \tag{14}$$

and by using Green's second identity, the domain integrals of function $\mathcal{F}(\mathbf{p},t)$ and the domain integral of scalar product $\boldsymbol{\mathcal{G}}(\mathbf{p},t) \cdot \nabla \mathcal{F}(\mathbf{p},t)$ ($\boldsymbol{\mathcal{G}}$ presents an arbitrary vector-valued function) weighted with the Green function T^* over Ω approximately transform into a finite set of N integrals over the boundary Γ

$$\int_\Omega \mathcal{F}\, T^*\, d\Omega \approx \Psi_n(\mathbf{s})\, \tilde{\Psi}_{nm}^p\, \mathcal{F}(\mathbf{p}_m,t), \tag{15}$$

$$\int_\Omega \boldsymbol{\mathcal{G}} \cdot \nabla \mathcal{F}\, T^*\, d\Omega \approx \Psi_n(\mathbf{s})\, \tilde{\Psi}_{nu}^p\, \boldsymbol{\mathcal{G}}(\mathbf{p}_{\underline{u}},t) \cdot \nabla \Psi_l^p(\mathbf{p}_u)\, \tilde{\Psi}_{lm}^p\, \mathcal{F}(\mathbf{p}_m,t); \tag{16}$$

$$\Psi_n(\mathbf{s}) = \int_\Gamma T^* \frac{\partial \hat{\Psi}_n^p}{\partial n_\Gamma}\, d\Gamma - \int_\Gamma \hat{\Psi}_n^p \frac{\partial T^*}{\partial n_\Gamma}\, d\Gamma - c^*(\Omega,\mathbf{s})\, \hat{\Psi}_n^p(\mathbf{s}). \tag{17}$$

The efficiency of the transformations (15,16) depends strongly on the choice of the interpolating functions Ψ_n^p. The so-called first order ($I_\Psi = 1$) radial interpolation functions are used in this paper

$$\Psi_n^p(\mathbf{p}) = \sum_{i_\Psi=0}^{I_\Psi} |\mathbf{p} - \mathbf{p}_n|^{i_\Psi}, \quad \hat{\Psi}_n^p(\mathbf{p}) = \sum_{i_\Psi=0}^{I_\Psi} \frac{|\mathbf{p} - \mathbf{p}_n|^{i_\Psi+2}}{(i_\Psi + 2)^2}. \tag{18}$$

The convergence properties of these interpolating functions have been studied by Yamada et al. [15] recently.

Integrals over time $[t_0, t_0 + \Delta t]$ appearing in equation (5) could be qualified into two types, illustrated by the scalar functions $\mathcal{E}$ and $\mathcal{F}$. By approximating these functions by linear time shape functions, the following approximative integrations are valid

$$\int_{t_0}^{t_0+\Delta t} \mathcal{E}\,\frac{\partial \mathcal{F}}{\partial t}\,dt \approx \mathcal{F}^{t_0+\Delta t}\,\frac{1}{2}\left(\mathcal{E}^{t_0+\Delta t} + \mathcal{E}^{t_0}\right) - \mathcal{F}^{t_0}\,\frac{1}{2}\left(\mathcal{E}^{t_0+\Delta t} + \mathcal{E}^{t_0}\right), \tag{19}$$

$$\int_{t_0}^{t_0+\Delta t} \mathcal{E}\,\mathcal{F}\,dt \approx \mathcal{F}^{t_0+\Delta t}\frac{\Delta t}{2}\left(\frac{2}{3}\,\mathcal{E}^{t_0+\Delta t} + \frac{1}{3}\,\mathcal{E}^{t_0}\right) + \mathcal{F}^{t_0}\frac{\Delta t}{2}\left(\frac{1}{3}\,\mathcal{E}^{t_0+\Delta t} + \frac{2}{3}\,\mathcal{E}^{t_0}\right), \tag{20}$$

where superscript denotes the evaluation at inital or final timestep level.

The boundary is discretized by N_Γ boundary elements Γ_k with piecewise straight-line geometry and piecewise constant space shape functions. The first N_Γ points $\mathbf{p}_n$ of the approximative function (18) coincide with the nodes (geometric centres) of the boundary elements, and the last N_Ω points are arbitrarily distributed in Ω. All subsequently involved boundary integrals have been evaluated analytically. Our previous studies show that for solidification problems, one can not expect much better behaviour of higher-order space shape functions due to the discontinuities of the heat fluxes at the phase-interface.

Equation (5) is solved by constructing an algebraic equation system of $j = 1, 2, \ldots, N$ equations. These equations are obtained by writing the discretized form of equation (5) for source point $\mathbf{s}$ to coincide with the nodal points $\mathbf{p}_n$. The deduced system of algebraic equations could be cast in a symbolic form

$$\mathrm{F}_{jm}^{t_0+\Delta t\,i}\,\mathcal{T}^i(\mathbf{p}_m, t_0 + \Delta t) + \mathbf{T}_{jm}^{t_0+\Delta t} \cdot \nabla \mathcal{T}^i(\mathbf{p}_m, t_0 + \Delta t)$$

$$= \mathrm{F}_{jm}^{t_0}\mathcal{T}(\mathbf{p}_m, t_0) + \mathbf{T}_{jm}^{t_0} \cdot \nabla \mathcal{T}(\mathbf{p}_m, t_0) + \mathrm{q}_{jm}^{t_0+\Delta t}\,q(\mathbf{p}_m, t_0 + \Delta t) + \mathrm{q}_{jm}^{t_0}\,q(\mathbf{p}_m, t_0), \tag{21}$$

which has to be rearranged according to boundary condition types before solution. The matrix elements are explicitly presented in [16].

The numerical solution of the nonlinear integral equation (5) inherently requires timestep iterations. Superscript i denotes the value of a quantity at the i-th iteration. The idea proposed by Voller and Swaminathan [17] has been used to some extent for the iterative updating of nonlinear terms with $\mathbf{\Lambda}$ and Υ. Since function $\mathcal{E}$ in equations (19,20) depends on function $\mathcal{F}$, the following approximation for function $\mathcal{E}$ at time level $t_0 + \Delta t$ at iteration level i has been included to speed up the internal timestep convergence

$$\mathcal{E}^{t_0+\Delta t\,i} = \mathcal{E}^{t_0+\Delta t\,i-1} + \frac{\partial \mathcal{E}}{\partial \mathcal{F}}^{t_0+\Delta t\,i-1}\left(\mathcal{F}^{t_0+\Delta t\,i} - \mathcal{F}^{t_0+\Delta t\,i-1}\right) \tag{22}$$

This strategy requires no under or overrelaxation. The timestep iterations are stopped when the absolute Kirchhoff variable difference of the two successive iterations does not exceed some predetermined positive margin $\mathcal{T}_\delta$ in any of the nodal points $\mathbf{p}_m$.

Numerical Examples

The characteristics of the developed method are checked by comparing the numerical solution with the closed form solution. To the best of the authors' knowledge the exact closed form solution exists only for a relatively simple steady state class of problems with uniform velocity field, i.e. the domain Ω is described by the cartesian coordinates $x_- < x < x_+$ and $y_- < y < y_+$. The boundary conditions at x_- and at x_+ are of the Dirichlet type with uniform temperatures $T_{\Gamma-}$ and $T_{\Gamma}+$. Thermal insulation boundary conditions of the Neumann type are assumed at the boundaries $y = y_-$ and $y = y_+$. The material moves with the constant uniform velocity $\mathbf{V} = \mathbf{V}_{\mathcal{S}} = \mathbf{V}_{\mathcal{L}}$ with the components $V_x = V$ and $V_y = 0\,[\mathrm{m/s}]$. The isothermal melting temperature is between $T_{\Gamma-}$ and $T_{\Gamma+}$. The solid phase occupies the domain with $x_- \le x_{\mathcal{M}}$, and the liquid one the domain with $x_{\mathcal{M}} \le x_+$ for $T_{\Gamma+} > T_{\Gamma-}$. The corresponding temperature distribution in phase $\mathcal{P}$ is

$$T_{\mathcal{P}}(x,y) = -\frac{\alpha_{\mathcal{P}}}{V_x}\exp\Big(\frac{V_x}{\alpha_{\mathcal{P}}}\,x + A_{\mathcal{P}}\Big) + B_{\mathcal{P}},\quad \alpha_{\mathcal{P}} = \frac{k_{\mathcal{P}}}{\rho_{\mathcal{P}}\,c_{\mathcal{P}}};\quad \mathcal{P} = \mathcal{S},\mathcal{L}. \tag{23}$$

with constants

$$A_{\mathcal{S}} = \log\Big(\frac{\frac{V_x}{\alpha_{\mathcal{S}}}(T_{\Gamma-} - T_{\mathcal{M}})}{\exp(\frac{V_x}{\alpha_{\mathcal{S}}}\,x_{\mathcal{M}}) - \exp(\frac{V_x}{\alpha_{\mathcal{S}}}\,x_-)}\Big),\quad A_{\mathcal{L}} = \log\Big(\frac{\frac{V_x}{\alpha_{\mathcal{S}}}(T_{\Gamma+} - T_{\mathcal{M}})}{\exp(\frac{V_x}{\alpha_{\mathcal{S}}}\,x_{\mathcal{M}}) - \exp(\frac{V_x}{\alpha_{\mathcal{S}}}\,x_+)}\Big),$$

$$B_{\mathcal{P}} = T_{\mathcal{M}} + \frac{\alpha_{\mathcal{P}}}{V_x}\exp\Big(\frac{V_x}{\alpha_{\mathcal{P}}}\,x_{\mathcal{M}} + A_{\mathcal{P}}\Big);\quad \mathcal{P} = \mathcal{S},\mathcal{L}, \tag{24}$$

and the position of the interphase boundary $x_{\mathcal{M}}$ determined from the transcendental equation

$$-\,\rho_0\,h_{\mathcal{M}}\,V_x = -k_{\mathcal{L}}\frac{\partial}{\partial x}T_{\mathcal{L}}(x_{\mathcal{M}},y) + k_{\mathcal{S}}\frac{\partial}{\partial x}T_{\mathcal{S}}(x_{\mathcal{M}},y). \tag{25}$$

The analytical solution is presented for the constant and different material properties (except density) of the phases, however the testing of the method is done with the unit thermal properties $\rho_0 = 1\,[\mathrm{kg/m^3}]$, $k = k_{\mathcal{S}} = k_{\mathcal{L}} = 1\,[\mathrm{W/(mK)}]$, $c = c_{\mathcal{S}} = c_{\mathcal{L}} = 1\,[\mathrm{J/(kgK)}]$. The adjacent constant thermal diffusivity is denoted by α. The isothermal melting temperature is approximated by a narrow temperature range $T_{\mathcal{S}} = 0.765\,[\mathrm{K}], T_{\mathcal{L}} = 0.775\,[\mathrm{K}]$ and linear variation of the liquid fraction function over this temperature interval. The computations are done on two meshes. Their schematics are shown on Figure 1. The steady-state solution was reached through a transient from the initial uniform temperature $T_0 = T_{\Gamma}-$ and a jump of the boundary condition at $x+$ from $T_{\Gamma-} = 0\,[\mathrm{K}]$ to $T_{\Gamma+} = 1\,[\mathrm{K}]$ for $t > t_0$. The timestep iteration margin T_δ was set at $0.001\,[\mathrm{K}]$ and the steady state was assumed to be reached when the maximum gridpoint difference between two sucessive time steps did not exceed T_δ.

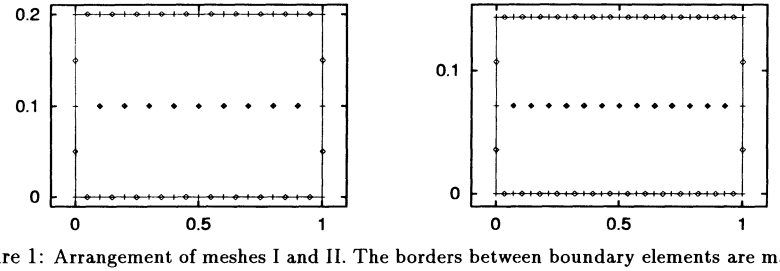

Figure 1: Arrangement of meshes I and II. The borders between boundary elements are marked with | and the gridpoints with ◇. Mesh I: $N = 33$, $N_\Gamma = 24$, $N_\Omega = 9$. Mesh II: $N = 45$, $N_\Gamma = 32$, $N_\Omega = 13$.

Because the one-dimensional problem is solved in two dimensions, the transversal length $y_+ - y_-$ becomes a free parameter. The solution behaves in an oscillatory manner if the transversal boundary element lengths are taken longer or shorter than the lateral ones. In such cases the first calculated temperatures in internal points after the initial temperature jump were below and those on the lateral sides above the exact solution. The behavior of the error in next time step was found to be reversed and its magnitude greater. The timestep length was changed in the interval from 0.005 [s] to 0.1 [s]. Shorter timesteps give larger amplitude growth of the oscillations. Same behavior has been observed also for the much simple conduction-only single-phase governed cases. The solution was found to be stable with equal length boundary elements. Global errors of the solution converge with shorter boundary elements as illustrated in Tables 1 and 2. The solution is not sensitive to timestep length changes.

Sensitivity with respect to Peclet number

In the first test case, the accuracy of the method was investigated with respect to the Peclet number $\mathrm{Pe} = V_x\,(x_+ - x_-)/\alpha$ on two different meshes by assumming the constant Stefan number $\mathrm{Ste} = \rho_0\, c\,(T_{\Gamma+} - T_{\Gamma-})/h_{\mathcal{M}}$.

Pe	1.0	2.0	3.0		10.0
T_{ave}[K]	.327E-2	.201E-2	.240E-2	.203E-2	.549E-2
T_{rms}[K]	.354E-2	.228E-2	.261E-2	.230E-2	.582E-2
T_{max}[K]	.460E-2	.369E-2	.345E-2	.372E-2	.833E-2
mesh	I	II	I	II	II

Table 1: Average, rms and maximum errors as a function of Peclet number. $\mathrm{Ste} = \infty$.

The respective errors of the steady-state solution have been calculated as

$$T_{\mathrm{ave}} = \frac{1}{N_\Omega}\sum_{n=1}^{N_\Omega} |T(\mathbf{p}_n - T_{\mathrm{ana}}(\mathbf{p}_n)|, \quad T_{\mathrm{rms}} = \sqrt{\frac{1}{N_\Omega}\sum_{n=1}^{N_\Omega} (\,T(\mathbf{p}_n) - T_{\mathrm{ana}}(\mathbf{p}_n)\,)^2},$$

$$T_{\mathrm{max}} = \max|T(\mathbf{p}_n) - T_{\mathrm{ana}}(\mathbf{p}_n)|; n = 1, 2, ..., N_\Omega, \tag{26}$$

where T_{cal} and T_{ana} stand for the numerical and analytical values respectively.

Sensitivity with respect to Stefan number

In the second test, the accuracy of the method with respect to the Stefan number has been investigated on two different meshes by assuming the constant Peclet number.

Ste	0.10	0.25	0.5		1.00
T_{ave}[K]	.332E-2	.306E-2	.272E-2	.260E-2	.245E-2
T_{rms}[K]	.359E-2	.331E-2	.296E-2	.280E-2	.267E-2
T_{max}[K]	.466E-2	.433E-2	.389E-2	.429E-2	.353E-2
mesh	I	I	I	II	I

Table 2: Average, rms and maximum errors in meshpoints as a function of Stefan number. $\mathrm{Pe} = 3$.

The computer times for solving one iteration on meshes I and II are approximately 10 and 14 CPU seconds respectively on a 100 MHz HP 715/100 workstation with an HP Fortran compiler.

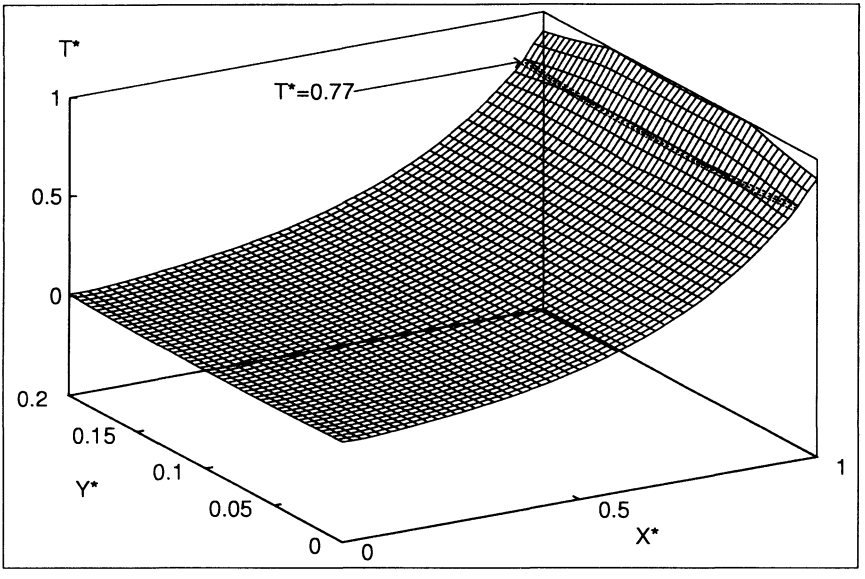

Figure 2: Axonometric view of the solution. Mesh I. Pe = 3, Ste = 1. Dimensionless scales are simply $T^* = T/(1\,[K])$, $X^* = x/(1\,[m])$, and $Y^* = y/(1\,[m])$.

Conclusions

This paper presents the first attempts to computationally solve the enthalpy equation relevant to solid-liquid phase change by assuming both convective and diffusive terms through the calculations that reduce to the integration of the fixed boundary quantities only. These types of problems appear for example during the continuous casting process with the velocity field beeing the result of the advection, and thermal, compositional, and surface tension driven convection. The current results confirm the suitability of the described method for problems with uniform velocity fields, e.g. for coping with advection in the presented example.

The principal advantage of the method is the ease of coping with geometrically complicated situations, ease of implementation of different boundary condition types, same order of temperature and heat flux approximation at the boundary, accuracy, and simple mesh structure. The main disadvantage of the method is the resulting large algebraic system of equations and relatively involved calculation of the domain integrals by the finite set of boundary ones.

Further elaboration of the developed method will concentrate on situations including nonuniform velocity fields. However, no exact solution is available for the spatially varying velocity field and melting/freezing, so the checking of the method and the model will have to rely on experimental data or results obtained by other numerical methods.

Acknowledgements

The work described in this paper is a part of the project Two-Fluid Modelling of Solidification. The authors would like to acknowledge the Ministry of Science and Technology of the Republic of Slovenia for support. The calculations in this paper were made on a workstation granted by the International Bureau, Jülich Research Centre, Germany in the framework of the joint German-Slovene bilateral research project Solidification Modelling by BEM.

References

[1] Yao, L.S. and Prusa, J. Melting and Freezing, Hartnett, J.P. (ed.), *Advances in Heat Transfer Vol.19*, Academic Press, New York, pp.1-95, 1989.

[2] Šarler, B. Bibliography on Stefan problem-1994, LFDT, Faculty of Mechanical Engineering Technical Report, University of Ljubljana, Ljubljana, 1994.

[3] NI, J. and Beckermann, C. A volume averaged two-phase model for transport phenomena during solidification, *Met.Trans.*, Vol.22B, pp.349-361, 1991.

[4] Voller, V.R. and Brent, A.D. The modelling of heat, mass and solute transport in solidification systems, *Int.J.Heat Mass Transfer*, Vol.32, pp.1719-1731, 1989.

[5] Wrobel, L.C. and Brebbia, C.A. An overview of boundary element applications to nonlinear heat transfer problems, Wriggers, P., Wagner, W. (eds.), *Nonlinear Computational Mechanics - State of the Art*, Springer-Verlag Berlin and New York, pp.226-239, 1991.

[6] Šarler, B., Mavko, B. and Kuhn, G. A Survey of the Attempts for the Solution of Solid-Liquid Phase Change Problems by the Boundary Element Method, Chapter 16, *Computational Methods for Free and Moving Boundary Problems in Heat and Fluid Flow*, Wrobel, L.C. and Brebbia, C.A. (eds.) Computational Engineering Series, Elsevier Applied Science, London, pp.373-400, 1993.

[7] Šarler, B., Mavko, B. and Kuhn, G. A BEM formulation for mass, momentum, energy and species transport in binary solid-liquid phase change systems, *Z.angew.Math.Mech.*, Vol.73, pp.T868-T873, 1993.

[8] Partridge, P.W., Brebbia, C.A. and Wrobel, L.C. *The Dual Reciprocity Boundary Element Method*, Computational Mechanics Publications and Elsevier Applied Science, Southampton and London, 1992.

[9] Šarler, B. and Košir, A. Application of the dual reciprocity method on Stefan problems, Wrobel, L.C. and Brebbia, C.A. (eds.) *Computational Modelling of Free and Moving Boundary Problems II*, Computational Mechanics Publications, Southampton, Elsevier Applied Science, London, pp.303-310, 1993.

[10] Šarler, B., Košir, A. and Kuhn, G. Dual reciprocity boundary element method for Stefan problems, *Int.J.Numer.Methods Eng.*, 1994, (submitted).

[11] Rathjen, K.A. and Jiji, L.M. Heat conduction with melting or freezing in a corner, *J.Heat Transfer*, Vol.93, pp.101-109, 1971.

[12] Dalhuijsen A.L. and Segal, A. Comparison of finite element techniques for solidification problems, *Int.J.Numer.Methods Eng.*, Vol.23, pp.1807-1829, 1986.

[13] Wrobel, L.C. and DeFiguieredo, D.B. A dual reciprocity boundary element formulation for convection-diffusion problems with variable velocity fields, *Eng.Anal.*, Vol.8, pp.312-319, 1990.

[14] Šarler, B., Mavko, B. and Kuhn, G. Mixture continuum formulation of convection-conduction energy transport in multiconstituent solid-liquid phase change systems for BEM solution techniques, *Eng.Anal.*, Vol.11, pp.109-117, 1993.

[15] Yamada, T., Wrobel, L.C. and Power, H. On the convergence of the dual reciprocity boundary element method, *Eng.Anal.*, Vol.13, pp.291-298, 1994.

[16] Šarler, B. and Košir, A. Solution of melting and solidification problems by the dual reciprocity boundary element method, Lewis, R.W. (ed.) *Numerical Methods in Thermal Problems VIII*, Pineridge Press, Swansea, pp.139-150, 1993.

[17] Voller, V.R. and Swaminathan, C.R. General source-based method for solidification phase change, *Num.Heat Transfer*, Vol.19B, pp.175-189, 1991.